Earth and Planetary Science Letters 545 (2020) 116403

Contents lists available at ScienceDirect

Earth and Planetary Science Letters

www.elsevier.com/locate/epsl

Towards understanding the origin of massive dolostones

Meng Ning [a], Xianguo Lang [b], Kangjun Huang [c], Chao Li [d], Tianzheng Huang [a], Honglin Yuan [c], Chaochao Xing [a], Runyu Yang [a], Bing Shen [a,*]

[a] Key Laboratory of Orogenic Belts and Crustal Evolution, MOE, School of Earth and Space Sciences, Peking University, Beijing, China
[b] State Key Laboratory of Oil and Gas Reservoir Geology and Exploitation & Institute of Sedimentary Geology, Chengdu University of Technology, Chengdu, China
[c] State Key Laboratory of Continental Dynamics and Shannxi Key Laboratory of Early Life and Environment, Department of Geology, Northwest University, Xi'an, China
[d] National Research Center for Geoanalysis, Chinese Academy of Geological Sciences, Beijing, China

ARTICLE INFO

Article history:
Received 20 January 2020
Received in revised form 9 May 2020
Accepted 5 June 2020
Available online 17 June 2020
Editor: F. Moynier

Keywords:
Dolomite Problem
magnesium isotope
sea level change
sedimentary cycles
South China
Cambrian

ABSTRACT

The origin of ancient massive dolostones, i.e. continuous dolostone sequence with a thickness >100 m and a platform-wide distribution, is the key issue of the 'Dolomite Problem' that cannot be clearly demonstrated by any existing dolomitization model individually or sequentially. It has been proposed that the massive dolostone could be generated by the stacking of multistage dolomitization events linked to the sea-level fluctuation, which results in repeatedly occurring of limestone precipitation-dolomitization cycles. However, the sequence of dolomitization events cannot be differentiated by any sedimentological or traditional geochemical techniques. Here we report Mg isotopic compositions of the massive dolostone ($\delta^{26}Mg_{dol}$) from the middle Cambrian Qinjiamiao Formation (QJM) in the Yangtze Platform, South China, which consists of cyclic depositions of shoaling upward sequences. The stratigraphic variation of $\delta^{26}Mg_{dol}$ is coincident with the depositional cycles, suggesting the dolomitization might be periodic and be coupled with the sea-level oscillation. As dolomitization fluids experience changes in $\delta^{26}Mg$ values during dolomitization processes, the intra-cycle stratigraphic $\delta^{26}Mg_{dol}$ profile reflects the processes of dolomitization. Our study indicates that the massive dolostone could be generated by the temporal and spatial stacking of multiple dolomitization events that are associated with sea-level fluctuation. If this model can be verified by other massive dolostone successions, the origin of massive dolostone may be resolved.

1. Introduction

Dolomite, one of the most enigmatic minerals, is abundant in pre-Cenozoic strata but rare in Cenozoic and modern sediments. It is hypothesized that such sharp contrast of dolomite distribution might be linked to the changes of environmental conditions, although factors controlling dolomite precipitation in the global scale remains elusive (Burns et al., 2000). The 'Dolomite Problem' (Fairbridge, 1957) refers to the sharp distinctions between ancient dolostone and modern dolomite in the spatial distribution, stratigraphic thickness and degree of crystal ordering (Kaczmarek and Sibley, 2011; Lumsden and Caudle, 2001; Mresah, 1998) (Table S1), and has puzzled geologists for more than 200 years (Warren, 2000). The 'Dolomite Problem' includes two key aspects: (1) How dolomite could precipitate from natural aqueous environment, since Mg^{2+} hydration inhibits dolomite precipitation (Lippmann, 1982). (2) How ancient 'massive dolostone', referring to continuous dolostone deposition with hundreds to thousands meters in thickness and hundreds of thousands square kilometers in area (or platform-wide distribution), could be formed, given modern dolomite is restricted in specific geographic environments and normally presents as thin layers (Arvidson and Mackenzie, 1999; Purser et al., 1994). In the case of the former, the energy barrier of Mg^{2+} hydration could be overcome by, e.g. an increase of Mg/Ca ratio of solution (Shinn et al., 1965), dilution of solution (Badiozamani, 1973), microbial or organic compound mediation (Roberts et al., 2013; Vasconcelos et al., 1995), or increase of ionic strength of fluid and with zinc complexation (Vandeginste et al., 2019). Therefore, although the exact pathways of dolomitization remain unclear, precipitation of dolomite at Earth's surface temperatures and pressures is entirely possible. On the other hand, various models, including the sabkha distilation (Shinn et al., 1965), brine reflux (Adams and Rhodes, 1960), burial diagenesis (Mattes et al., 1980), thermogenesis (Davies and Smith, 2006) and organogensis (Vasconcelos et al., 1995) models, have been proposed to inter-

* Corresponding author.
E-mail address: bingshen@pku.edu.cn (B. Shen).

https://doi.org/10.1016/j.epsl.2020.116403
0012-821X/

pret the formation of modern dolomite. However, the application of these models individually or sequentially to interpret ancient massive dolostone is difficult (Kaczmarek et al., 2017; Land, 1985; Machel, 2004). For example, it remains unclear whether massive dolostone formation involves with a single or multiple dolomitization events or how to recognize/sequence the dolomitization events in the stratigraphic record. Neither is known about the Mg source or the mechanism that effectively pumps Mg into thick carbonate deposits in the platform scale.

Therefore, the origin of ancient massive dolostone is an important yet unresolved part of the 'Dolomite Problem' (Land, 1985; Machel, 2004; Warren, 2000). It is typically a consensus that ancient massive dolostone was generated by the replacement of Ca-carbonate precursors (Kaczmarek et al., 2017; Land, 1985; Machel, 2004). Massive dolostone formation not only needs to overcome the kinetic barrier imposed by Mg^{2+} hydration, but also requires sufficient Mg-bearing fluids and a long-term Mg pumping mechanism. Obviously, a single dolomitization event is hard to envision for the extensive dolomite formation in a large carbonate platform. Lumsden and Caudle (2001) proposed that massive dolostone could be generated by stacking of multiple episodes of dolomitization events that are linked to sea-level fluctuation. This model seems reasonable, because most ancient massive dolostones are composed of cyclic depositions of shoaling upward sequences (e.g. massive dolostone in the Alpine Triassic (Meister et al., 2013)). In addition, Kah et al. (2000) reported progressive enrichment of ^{18}O from subtidal to supratidal (exposed) dolostone of the Mesoproterozoic Social Cliff Formation, reflecting the sea-level driven environmental changes. Yet, dolomitization in massive dolostone has not been unambiguously sequenced by sedimentological or geochemical approaches.

In this study, we use Mg isotope to constrain the sequence of dolomitization events in a succession of Cambrian massive dolostone in South China. Compared with other techniques, Mg isotope analysis has several advantages in the study of dolomite/dolostone. Firstly, the major Mg reservoirs in the surface Earth display a wide range of variation in Mg isotopic composition (Higgins and Schrag, 2010, 2015; Teng, 2017; Tipper et al., 2006, 2010; Wimpenny et al., 2014), allowing using Mg isotopes to trace the Mg source. Secondly, the isotopic fractionation during dolomite precipitation at room temperature has been precisely determined (Fantle and Higgins, 2014; Higgins and Schrag, 2015; Li et al., 2015). Thirdly, Mg isotopic compositions of dolostone are controlled by the dolomitization processes, and numerical models for Mg isotope systematics of dolomitization have been established (Huang et al., 2015; Peng et al., 2016), providing the theoretical frameworks for the study of ancient massive dolostone.

In order to further constrain the 'Dolomite Problem', we measured Mg isotopic compositions of massive dolostone from the middle Cambrian Qinjiamiao (QJM) Formation in the Yangtze Platform, South China (Fig. S1). Combining with the detailed sedimentological analyses, the sequence of dolomitization events was identified, and a model for massive dolostone formation is proposed.

2. Sedimentological background of the QJM dolostone

The middle to late Cambrian succession is mainly composed of massive dolostone, and is represented by the Loushanguan Group in the Upper Yangtze Region (Guizhou Province and its adjacent areas) (Mei, 2007), and by the Qinjiamiao (~300 m thick) and Sanyoudong formations (~300 m thick) in the Yangtze Gorges area. This dolostone succession has a thickness ranging from several hundreds to more than one thousand meters across an area of ~500,000 square kilometers (Fig. S1).

We analyzed the Member I of the QJM Formation at the Liujiachang section (See supplementary material for detail), which is composed of variably dolomitized subtidal ooid grainstone, intertidal wackestone to packstone with algal fabric, and supratidal dolomicrite with gypsum pseudomorphs (Fig S3). Detailed facies analysis recognized eight lithofacies and three facies associations (subtidal, intertidal and supratidal) (Fig. 1 and Table S2), suggesting the deposition in a tidal flat with periodic siliciclastic input (Fig. S3 and supplementary material).

The lithofacies sequence in Cycle 1 consists of L6-L4-L2 in ascending order, indicating an intertidal to supratidal deposition. Cycle 2 and cycle 3 consist of lithofacies L8-L4-L2 and L7-L4-L2 respectively, and both record the deposition from subtidal to supratidal environment. Cycle 4 and cycle 5 consist of lithofacies L4-L3 and L5-L1, representing deposits of lower intertidal to supratidal environment. Cycle 6 is composed of L4-L3-L2-L1 lithofacies and cycle 7 consists of lithofacies L3-L2-L1. Both cycles represent the upper intertidal to supratidal deposition.

The stacking of these cycles indicates frequent sea-level oscillation at parasequence scales. Decimeter-scale stratigraphic facies changes suggest a high frequency and low amplitude of sea-level fluctuation (Yang and Kominz, 2003). Cycles 2 and 3 include a complete depositional cycle starting from subtidal and passing into intertidal and supratidal facies upward, and defines the largest magnitude of sea-level change. Cycles 1, 4 and 5, characterized by the absence of subtidal lithofacies, may imply a relatively constant sea-level during initial regression period or a small degree of sea-level change. Cycles 6 and 7 represent the subsequent progradation of peritidal flat and intense evaporation during a stage of relatively low sea-level.

3. Materials and methods

Sample preparation. Dolostone samples were collected nearly continuously in a 3.2-m interval at the Liujiachang section, Hubei province. Mirrored thin and thick sections were prepared for petrographic analyses and micro-drill sampling, respectively. Powder samples were drilled from thick sections under the guidance of petrographic observation in the corresponding thin sections. Approximately 10 mg powder of each sample was dissolved by 10 mL 0.5 N acetic acid in an ultrasonic bath for 30 min at 50 °C. After centrifugation, supernatant was prepared for elemental and magnesium isotope analysis.

Major and trace elements analysis. Elemental composition was determined by a Spectro Blue Sop inductively coupled plasma optical emission spectrometer (ICP-OES) fitted with a Water Cross-flow nebulize at Peking University. The detailed analytical procedure has been reported in previous publications (Huang et al., 2015), and will not be iterated here. The analytical precession for major and minor elements (e.g. Ca, Mg, Fe, Mn, K, Na, etc.) are better than 5%. In order to determine the Mg purification procedure and evaluate the efficiency of column chromatography, major and trace elements analysis was conducted before and after Mg purification.

Magnesium isotope analysis. Mg was purified by cation-exchange chromatography using an established two-stage column procedure (Bao et al., 2019; Huang et al., 2015). After purification, Ca/Mg, Al/Mg, Na/Mg, K/Mg, and Fe/Mg are less than 0.05, and Mg recovery is better than 99%. Mg isotope ratios were measured on a Nu plasma Multi-Collector Inductively Coupled Plasma Mass Spectrometer (MC-ICP-MS) in State Key Laboratory of Continental Dynamics at Northwest University, China and a Thermo Scientific Neptune MC-ICP-MS at National Research Center for Geoanalysis, Chinese Academy of Geological Sciences, China. Mg isotope values are reported in δ-notation as per mil deviation relative to the

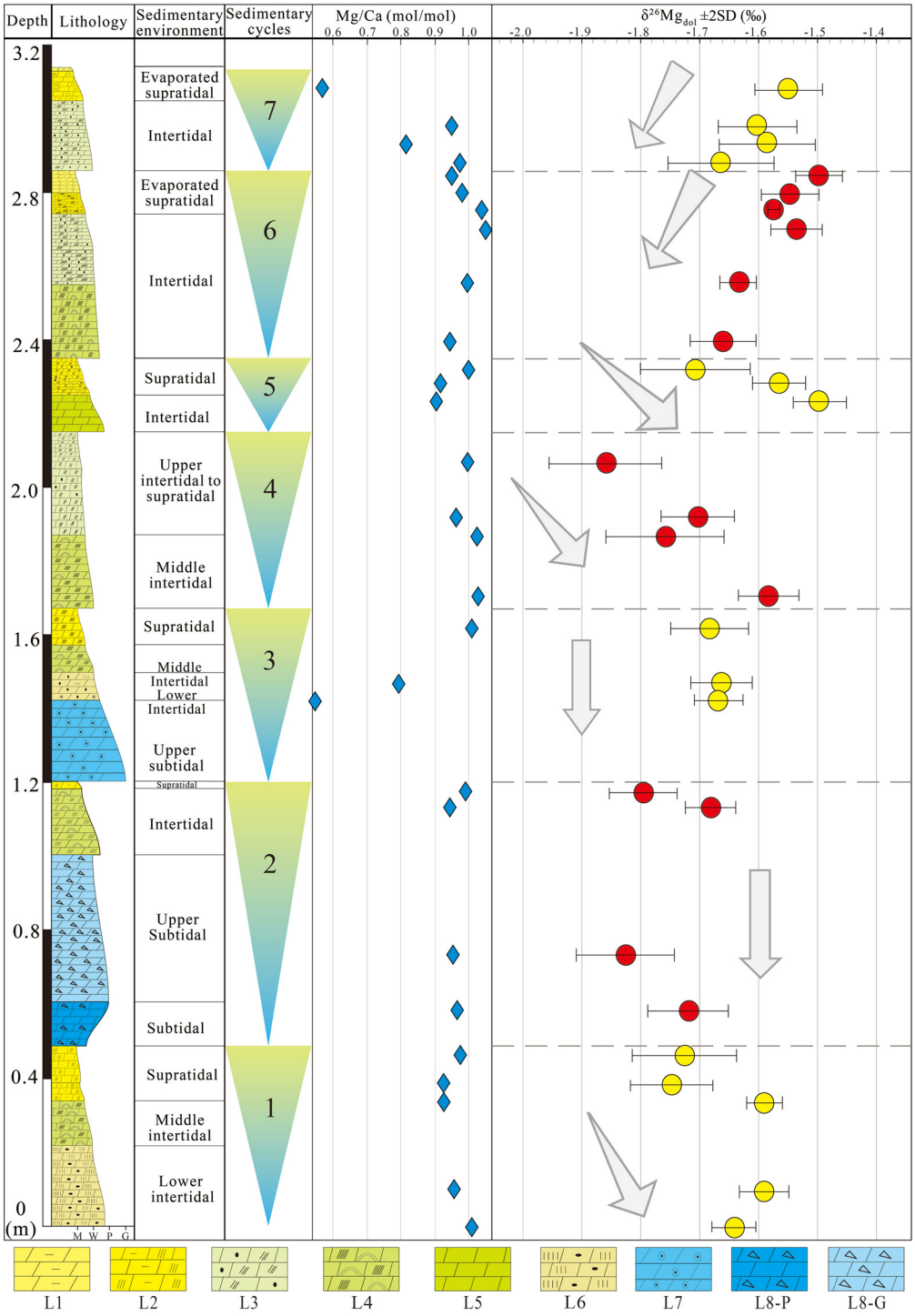

Fig. 1. The stratigraphic profiles of $\delta^{26}Mg_{dol}$ and sedimentary cycles of the studied section of the Qinjiamiao Formation in the Liujiachang section, showing the coupling of stratigraphic variation of $\delta^{26}Mg_{dol}$ and sedimentary cycles (see the supplementary materials for legend codes interpretation).

standard DSM3: $\delta^{26}Mg = [(\delta^{x}Mg/^{24}Mg)_{sample}/(\delta^{x}Mg/^{24}Mg)_{DSM3} - 1] \times 1000$, where x refers to mass 25 or 26. The reproducibility of Mg isotope measurements was assessed by using synthetic GSB-Mg-Ca mixed standard solution with different Mg/Ca ratios and USGS reference materials BHVO-2 and BCR-2. Multiple analyses of GSB-Mg yield $\delta^{26}Mg$ value of -2.01‰ ~2.04‰, which is consistent with the recommended value of -2.04±0.04‰ (Bao et al., 2019; Ke et al., 2016). Results for BHVO-2 (-0.26‰±0.04‰) and BCR-2 (-0.16‰±0.09‰) are also consistent with recommended values (BHVO-2: -0.24±0.08‰, BCR-2: -0.16±0.01‰ to -0.33±0.04‰) (Teng, 2017).

4. Results

Mg isotopic compositions ($\delta^{26}Mg_{dol}$) of the QJM dolostones range from -1.85‰ to -1.49‰ (Figs. 1, S4, Table S3). The stratigraphic variation of $\delta^{26}Mg_{dol}$ is broadly coincident with the depositional cycles (Fig. 1). Three types of $\delta^{26}Mg_{dol}$ profile are observed within individual sedimentary cycle, i.e. the downward decreasing trend (Cycle 6 and 7), the downward increasing trend (Cycle 1, 4 and 5) and vertically invariant of $\delta^{26}Mg_{dol}$ (Cycle 2 and 3). $\delta^{26}Mg_{dol}$ profile of Cycle 1 displays a slightly downward increasing trend from -1.74‰ to -1.59‰, while $\delta^{26}Mg_{dol}$ of cycles 2

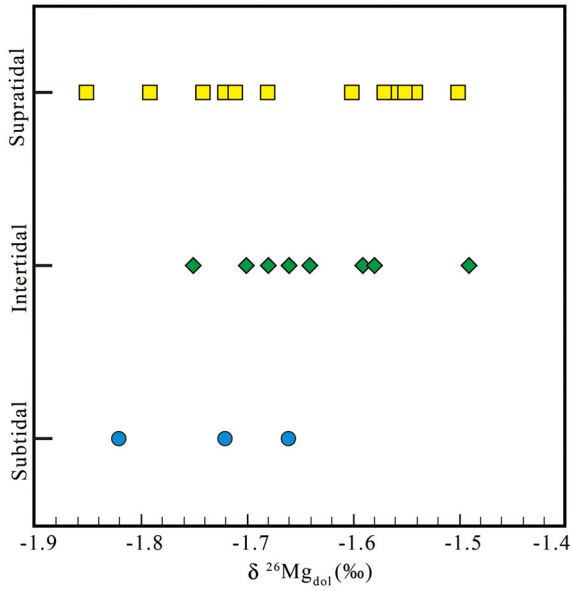

Fig. 2. $\delta^{26}Mg_{dol}$ variation of dolostone from different sedimentary environments.

and 3 remains nearly invariant (oscillating between -1.68‰ and -1.82‰, and between -1.66‰ and -1.68‰, respectively). $\delta^{26}Mg_{dol}$ profiles of cycles 4 and 5 display significant downward enrichment of ^{26}Mg, increasing from -1.85‰ to -1.58‰ and from -1.71‰ to -1.49‰, respectively. In contrast, cycles 6 and 7 demonstrate the downward decreasing trends with $\delta^{26}Mg_{dol}$ decreasing from -1.50‰ to -1.66‰ and from -1.55‰ to -1.66‰, respectively.

5. Discussion

5.1. Evaluation of intra-cycle variation of Mg isotopes

Several lines of evidence suggest the stratigraphic variation of $\delta^{26}Mg_{dol}$ record the pristine signals of dolomitization. First, previous studies indicate that $\delta^{26}Mg_{dol}$ is not sensitive to post-depositional diagenetic alteration and low grade metamorphism (Geske et al., 2012; Hu et al., 2019; Li et al., 2019). Second, though different mixing between calcite and dolomite in partially dolomitized samples may result in the variation of $\delta^{26}Mg_{dol}$ (Peng et al., 2016), completely dolomitized QJM dolostone evidenced by consistent Mg/Ca (mole/mole) ratios (∼1) argue against various degrees of dolomitization (Fig. 1, Table S3). Third, $\delta^{26}Mg_{dol}$ variation is not sensitive to dolomite crystal types, because dolomites with different crystal morphologies share similar $\delta^{26}Mg$ values (Huang et al., 2015; Ning et al., 2019). Fourth, different depositional facies (i.e. subtidal, intertidal, supratidal) have overlapping range of $\delta^{26}Mg_{dol}$ values (Fig. 2), suggesting that the stratigraphic variation of $\delta^{26}Mg_{dol}$ is not controlled by sedimentary facies either.

On the other hand, $\delta^{26}Mg_{dol}$ values could be highly variable due to the fluctuation of local environments, such as sedimentation rate, migration rate of dolomitization fluids, and distance from the source of dolomitization fluids, etc. (Blättler et al., 2015; Higgins and Schrag, 2010; Huang et al., 2015; Peng et al., 2016). For the QJM dolostone, although there is no consistent trend within individual cycle, it is clear that the turning points of the $\delta^{26}Mg_{dol}$ profile (either value or stratigraphic trend) are coincident with the boundaries of depositional cycles (Fig. 1). Even for cycles 2 and 3, both of which have invariant $\delta^{26}Mg_{dol}$ profile, $\delta^{26}Mg_{dol}$ values of Cycle 3 are systematically higher (by ∼ 0.1‰) than those of Cycle 2.

Thus, the stratigraphic Mg isotopic variation trend may reflect the process of dolomitization (Huang et al., 2015; Mavromatis et al., 2014; Peng et al., 2016), and the coupling of $\delta^{26}Mg_{dol}$ profiles and sedimentary cycles indicates the linkage between dolomitization and sea-level fluctuation. Below we will explore how $\delta^{26}Mg_{dol}$ profile reflect the dolomitization processes.

5.2. Stratigraphic Mg isotopic profiles reflect dolomitization processes

Because of preferential incorporation of ^{24}Mg during dolomite formation (Blättler et al., 2015; Fantle and Higgins, 2014; Geske et al., 2015; Higgins and Schrag, 2010; Huang et al., 2015), dolomitization fluid becomes progressively enriched in ^{26}Mg as the dolomitization process proceeds, resulting in a higher value of $\delta^{26}Mg$ for the later formed dolomite (Huang et al., 2015). Thus, the vertical $\delta^{26}Mg_{dol}$ profile can be used to constrain the transportation of Mg in dolomitization and the evolution of Mg isotopic composition of dolomitization fluid ($\delta^{26}Mg_{df}$), and thus provide direct constraint on the process of dolomitization.

Dolomitization fluids could be transported downward resulting in the dolomitization of pre-existing calcite or aragonite. For example, the reflux dolomitization model (Adams and Rhodes, 1960) proposes that the dolomitization fluid is generated within a restricted lagoon or basin via evaporation, and the saline, Mg-enriched (i.e. high Mg/Ca ratio) brine could percolate into and dolomitize the underlying calcareous sediments (Machel, 2004). Locally, *in situ* percolation of dense brine fluid would cause a top-down dolomitization, i.e. dolomitization first occurs in the seafloor. Thus, dolomite formed at shallower depth of sediments would have lower $\delta^{26}Mg_{dol}$ than that formed at deep depth. The downward migration of fluids with high Mg/Ca ratio would thus result in a downward increasing trend of $\delta^{26}Mg_{dol}$ (Fig. 3A). This process can be quantified by the Advective Flow (AF) model (Fig. 3A) (Peng et al., 2016). Furthermore, the temporal change of $\delta^{26}Mg_{df}$ of source fluid would affect the absolute value of $\delta^{26}Mg_{dol}$, but will not modify the downward increasing trend of $\delta^{26}Mg_{dol}$ (Peng et al., 2016).

Alternatively, in the regional scale, the Mg-rich brine could also transport laterally within sediment along the gradient of hydrostatic pressure, resulting in the dolomitization away from the source of dolomitization fluid. In this process, $\delta^{26}Mg_{df}$ would change along the trajectory of fluid flow, but $\delta^{26}Mg_{dol}$ would be vertically invariant in each locality (Huang et al., 2015; Peng et al., 2016), i.e. the invariant vertical profile of $\delta^{26}Mg$ (Fig. 3B). Similarly, the invariant $\delta^{26}Mg_{dol}$ profile is not affected by the, e.g. change of $\delta^{26}Mg_{df}$, migration of source locality, and variation of fluid velocity, but the absolute value of $\delta^{26}Mg_{dol}$ would be affected (Peng et al., 2016).

For the penecontemporaneous dolomitization near the sediment-water interface (SWI), dolomitization is concurrent with Ca-carbonate precipitation (Illing et al., 1965 and many others since this time). The seawater Mg diffuses downwards into sediments and results in a continuous dolomitization along with Ca-carbonate precipitation, collectively known as the seawater dolomitization process. Such process can be simulated by the diffusion-advection-reaction model (DAR) (Huang et al., 2015). Similar to the *in situ* reflux process, seawater Mg is downward transported into sediments. Though driven by different processes, the seawater dolomitization would also generate a downward increasing $\delta^{26}Mg_{dol}$ profile as well. If a steady state is applied, i.e. dolomitization of a thick sequence of succession, the lower portion would display invariant $\delta^{26}Mg_{dol}$ profile, because dolomitization would be terminated when limestone is completely converted to dolostone (Huang et al., 2015). Thus, $\delta^{26}Mg_{dol}$ of seawater dolomitization would be characterized by a downward increasing in the top and invariant values in the bottom, if $\delta^{26}Mg_{df}$ remains a constant.

In addition to the trajectory of dolomitization fluid, stratigraphic trend of $\delta^{26}Mg_{dol}$ for the seawater dolomitization may also

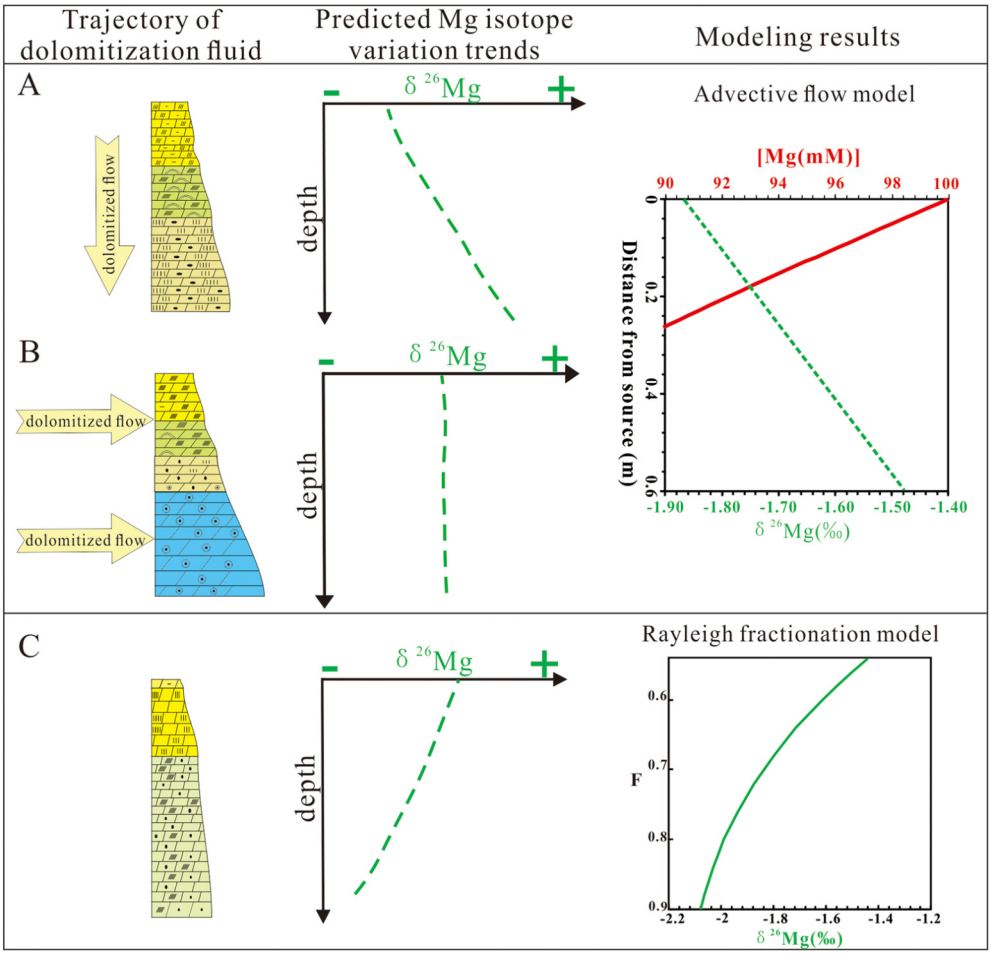

Fig. 3. Prediction and modeling results showing the vertical $\delta^{26}Mg_{dol}$ profile in different dolomitization processes. (A) The downward increase of $\delta^{26}Mg_{dol}$ with the dolomitization fluid reflux vertically from the seafloor. (B) The invariant vertical $\delta^{26}Mg_{dol}$ profile with lateral migration of the dolomitization fluid. (C) In a semi-closed system, the upward increase of $\delta^{26}Mg_{dol}$ represents the progressive enrichment of ^{26}Mg of seawater due to penecontemporaneous dolomitization.

result from the change of $\delta^{26}Mg_{df}$. This is particularly the case, when dolomitization occurs in a restricted or semi-restricted basin with periodic recharge of Mg, e.g. penecontemporaneous sabkha dolomitization. When dolomitization is the only major process removing seawater Mg, $\delta^{26}Mg_{df}$ evolves through time, and can be simulated by the Rayleigh fractionation model (see SI) (Fig. 3C). Thus, in this scenario the vertical profile of $\delta^{26}Mg_{dol}$ is controlled by both dolomitization process and the evolution of $\delta^{26}Mg_{df}$. The $\delta^{26}Mg_{dol}$ profile is dependent on sedimentation rate and the rate of $\delta^{26}Mg_{df}$ change. At a high sedimentation rate, small $\delta^{26}Mg_{dol}$ gradient would be generated in the dolomitization process (Huang et al., 2015), and the rapid change of $\delta^{26}Mg_{df}$ would result in a downward increasing trend of $\delta^{26}Mg_{dol}$. In contrast, a low sedimentation rate and/or a slow change of $\delta^{26}Mg_{df}$ would generate a downward decreasing trend of $\delta^{26}Mg_{dol}$.

5.3. Dolomitization process of the QJM massive dolostone

The coupling of $\delta^{26}Mg_{dol}$ profiles and sedimentary cycles (Fig. 1) implies the dolomitization processes of the QJM massive dolostone might be related to the sea-level oscillation. The migration of dolomitization fluids as well as the dolomitization processes can be constrained by the vertical profile of $\delta^{26}Mg_{dol}$. The downward increasing of $\delta^{26}Mg_{dol}$ observed in cycles 1, 4 and 5 implies a downward migration of dolomitization fluid, and dolomitization occurred after the deposition of supratidal sediments, i.e. in the top of depositional sequence. Possible dolomitization models include the *in situ* reflux model (Fig. 3A).

The invariant $\delta^{26}Mg_{dol}$ profile in cycles 2 and 3 indicates dolomitization fluid migrates laterally, which might be explained by the *ex situ* reflux dolomitization model (Fig. 3B), i.e. dolomitization driven by the lateral migration of dolomitization fluid (Jones and Rostron, 2000). Both cycles are composed of thick subtidal to intertidal lithofacies and relative thin supratidal lithofacies. Thus, dolomitization fluid might have sourced from adjacent shallower regions, e.g. supratidal environment where dolomitization fluid was generated. The *ex situ* dolomitization may not necessarily take place in the top of sedimentary cycle. Instead, dolomitization may significantly postdate Ca-carbonate precipitation, resulting in the simultaneous dolomitization of multiple cycles of deposits. It should be noted that no matter the process of dolomitization, $\delta^{26}Mg_{dol}$ of pre-existing dolomite would not be altered by later stage of dolomitization (Hu et al., 2019). At the QJM section, although both cycles 2 and 3 show invariant $\delta^{26}Mg_{dol}$ profiles, we suggest they have undergone two separate dolomitization events due to systematic higher $\delta^{26}Mg_{dol}$ values of the Cycle 3. Such differences may reflect, e.g., increase of $\delta^{26}Mg_{df}$, migration of fluid source toward the location, or slower flow rate of dolomitization fluid (Peng et al., 2016).

The downward decreasing trend of $\delta^{26}Mg_{dol}$ profile in cycles 6 and 7 can be explained by upward migration of dolomitization fluids, e.g. less dense Mg-rich hydrothermal fluid. However, hydrothermal dolomitization is not supported by the absence of hydrothermal veins or negligible recrystallization of the QJM dolostone (Fig. S3). Alternatively, this trend may reflect the variations

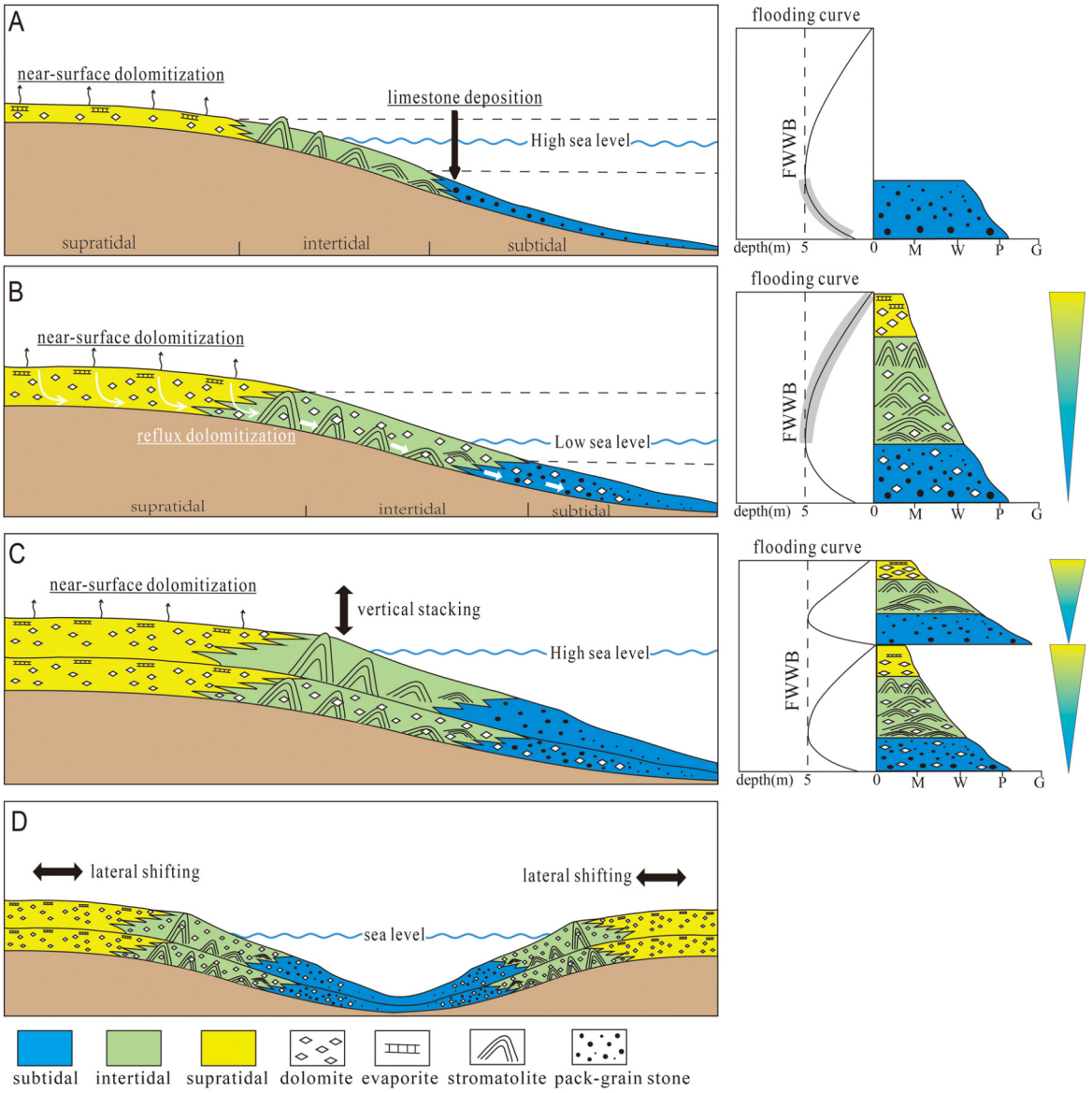

Fig. 4. The conceptual model of the massive dolostone formation. (A) At high sea-level, limestone is deposited in the subtidal to lower intertidal environment. (B) At low sea-level, dolomitization occurs in the upper-intertidal to supratidal environment, resulting in the replacement of Ca-carbonate that was deposited when the sea-level was high. The massive dolostone formation is directly linked to the fluctuation of sea-level, resulting in the vertical stacking (C) and lateral shifting (D) of dolomitization.

in $\delta^{26}Mg_{df}$ during penecontemporaneous dolomitization process. Presence of gypsum pseudomorphs in these two cycles suggests intense evaporation in a presumably (semi-) closed environment, where dolomitization would cause a progressive enrichment of ^{26}Mg in seawater.

Thus, Mg isotope data indicate that dolomitization might be periodic. We recognized three types of dolomitization processes that might be explained by the penecontemporaneous dolomitization, *in situ* reflux dolomitization, and *ex situ* reflux dolomitization. Dolomitization is favored at the top of each depositional cycle that is represented by the intertidal to supratidal depositional environment (Petrash et al., 2017). In this scenario, the cycle boundary might be collectively called the dolomitization window, whereas in other cases, e.g. seawater dolomitization, the cycle boundary marks the termination of contemporaneous dolomitization.

5.4. A solution to the origin of massive dolostone

Our study provides a possible solution to the formation of massive dolostone. Massive dolostone cannot be formed in a single dolomitization event. For example, in the reflux model, even with high Mg concentration of dolomitization fluid and high-permeability of calcareous sediments, the modeling results show that brines can only discharge into the platform top within 30 km away from their source and cannot extend over the length scales of hundreds of kilometers (Jones and Rostron, 2000). Instead, the coupling of $\delta^{26}Mg_{dol}$ profile and sedimentary cycles provides direct evidence in supporting the hypothesis of massive dolostone formation by the stacking of multiple episodes of dolomitization events linked to the sea-level fluctuations (Lumsden and Caudle, 2001).

We propose a model for the formation of massive dolostones (Fig. 4). At the relatively high sea-level, limestone precipitates in the subtidal or lower intertidal environment (Fig. 4A). When the sea-level drops, (partial) subaerial exposure that leads to a transition from subtidal to upper intertidal or supratidal environment would cause the near-surface dolomitization (Mresah, 1998), mainly dolomitization of pre-existing Ca-carbonate probably including some degrees of direct dolomite precipitation, e.g. organogenesis dolomite formation (Petrash et al., 2017) (Fig. 4B). Dolomitization fluid may percolate into the underlying porous sediments

to replace Ca-carbonate. The limestone precipitation - dolomitization cycle occurs repeatedly with the fluctuations of sea-level (Fig. 4C). Lateral migration of supratidal or intertidal zone allows dolomitization in a platform scale (Fig. 4D). Individual dolomitization event may be driven by different dolomitization processes depending on the local physio-chemical and hydrodynamic conditions. Overall, dolomitization is closely coupled with sea-level fluctuation, and the lateral migration and vertical stacking of sedimentary cycles would result in the platform-wide deposition of thick sequence of dolostone.

In sum, interpretation of massive dolostone does not require a new dolomitization model. Massive dolostone formation may include multiple dolomitization models, and the specific dolomitization model can be identified by the detailed sedimentary facies analysis and Mg isotope profile. For example, the *in situ* reflux model, characterized by the intertidal facies with a downward increasing of $\delta^{26}Mg_{dol}$, may switch to penecontemporaneous sabkha model, represented by evaporative supratidal facies with a downward decreasing of $\delta^{26}Mg_{dol}$, when sea-level falls. As Hardie in 1987 already stated, "there are dolomites and dolomites" (Hardie, 1987), no "one size fits all" dolomitization model could be applied to account for the formation of thick- to massive-bedded dolostone. Our study provides a testable solution for investigating massive dolostone formation on a case-to-case basis.

6. Conclusions

None of the existing dolomitization models can explain the origin of ancient massive dolostones of hundreds-meter thick with platform-wide distribution. We carried out detailed sedimentary facies and Mg isotope analysis of middle Cambrian massive dolostone (the QJM Formation) from South China. Facies analysis shows that the QJM massive dolostone is composed of multiple shoaling upward sedimentary cycles, each of which ranges from a few decimeters to several tens of meters in thickness. Mg isotopic compositions of the QJM dolostone indicate close coupling between dolomitization and sedimentary cycles. Dolomitization events could occur at the top of shoaling upward sequences, and each event might be responsible for the dolomitization of Ca-carbonate deposited in a single cycle. On the other hand, penecontemporaneous dolomitization might persist throughout the depositional cycle, but it terminates at the top of cycle. In addition, three types of dolomitization process can be identified based on the vertical $\delta^{26}Mg_{dol}$ profiles, suggesting diverse dolomitization processes might have involved in the massive dolostone formation. This study indicates that dolomitization of massive dolostone can be sequenced by a high-resolution Mg isotope data under a detailed sedimentary facies framework. If the coupling of sedimentary cycle and dolomitization events can be verified in other massive dolostone successions, the origin of massive dolostone would be resolved.

Declaration of competing interest

The authors declare that they have no known competing financial interests or personal relationships that could have appeared to influence the work reported in this paper.

Acknowledgements

We thank Yiwu Wang and Haiyang Luo for field assistance. We also thank Zhouqiao Zhao and Haoran Ma for laboratory assistance. Meng Ning would like to thank Judith Ann McKenzie for discussing 'Dolomite Problem' with her. The insightful comments of reviewer Linda Kah are much appreciated. We also thank the editor Frederic Moynier for a thorough review and editorial handling of the manuscript. This work was supported by the National Natural Science Foundation of China [grant numbers 41772359, 41602343 and 41802024].

Appendix A. Supplementary material

Supplementary material related to this article can be found online at https://doi.org/10.1016/j.epsl.2020.116403.

References

Adams, J.E., Rhodes, M.L., 1960. Dolomitization by seepage refluxion. Am. Assoc. Pet. Geol. Bull. 44, 1912–1920. https://doi.org/10.1306/0BDA6263-16BD-11D7-8645000102C1865D.

Arvidson, R.S., Mackenzie, F.T., 1999. The dolomite problem: control of precipitation kinetics by temperature and saturation state. Am. J. Sci. 299, 257–288. https://doi.org/10.2475/ajs.299.4.257.

Badiozamani, K., 1973. The dorag dolomitization model, application to the middle Ordovician of Wisconsin. J. Sediment. Res. 43, 965–984. https://doi.org/10.1306/74d728c9-2b21-11d7-8648000102c1865d.

Bao, Z., Huang, K., Huang, T., Shen, B., Zong, C., Chen, K.-Y., Yuan, H., 2019. Precise magnesium isotope analyses of high-K and low-Mg rocks by MC-ICP-MS. J. Anal. At. Spectrom. 34. https://doi.org/10.1039/C9JA00002J.

Blättler, C.L., Miller, N.R., Higgins, J.A., 2015. Mg and Ca isotope signatures of authigenic dolomite in siliceous deep-sea sediments. Earth Planet. Sci. Lett. 419, 32–42. https://doi.org/10.1016/j.epsl.2015.03.006.

Burns, S.J., Mckenzie, J.A., Vasconcelos, C., 2000. Dolomite formation and biogeochemical cycles in the Phanerozoic. Sedimentology 47, 49–61. https://doi.org/10.1046/j.1365-3091.2000.00004.x.

Davies, G.R., Smith, L.B., 2006. Structurally controlled hydrothermal dolomite reservoir facies: an overview. Am. Assoc. Pet. Geol. Bull. 90, 1641–1690. https://doi.org/10.1306/05220605164.

Fairbridge, R.W., 1957. The dolomite question. In: LeBlanc, R.J., Breeding, J.G. (Eds.), Regional Aspects of Carbonate Deposition SEPM Society for Sedimentary. Geology, Tulsa, OK, pp. 125–178.

Fantle, M.S., Higgins, J., 2014. The effects of diagenesis and dolomitization on Ca and Mg isotopes in marine platform carbonates: implications for the geochemical cycles of Ca and Mg. Geochim. Cosmochim. Acta 142, 458–481. https://doi.org/10.1016/j.gca.2014.07.025.

Geske, A., Goldstein, R.H., Mavromatis, V., Richter, D.K., Buhl, D., Kluge, T., John, C.M., Immenhauser, A., 2015. The magnesium isotope (δ^{26}Mg) signature of dolomites. Geochim. Cosmochim. Acta 149, 131–151. https://doi.org/10.1016/j.gca.2014.11.003.

Geske, A., Zorlu, J., Richter, D.K., Buhl, D., Niedermayr, A., Immenhauser, A., 2012. Impact of diagenesis and low grade metamorphosis on isotope (δ^{26}Mg, δ^{13}C, δ^{18}O and ^{87}Sr/^{86}Sr) and elemental (Ca, Mg, Mn, Fe and Sr) signatures of Triassic sabkha dolomites. Chem. Geol. 332–333, 45–64. https://doi.org/10.1016/j.chemgeo.2012.09.014.

Hardie, L.A., 1987. Dolomitization; a critical view of some current views. J. Sediment. Res. 57, 166–183. https://doi.org/10.1306/212f8ad5-2b24-11d7-8648000102c1865d.

Higgins, J.A., Schrag, D.P., 2010. Constraining magnesium cycling in marine sediments using magnesium isotopes. Geochim. Cosmochim. Acta 74, 5039–5053. https://doi.org/10.1016/j.gca.2010.05.019.

Higgins, J.A., Schrag, D.P., 2015. The Mg isotopic composition of Cenozoic seawater – evidence for a link between Mg-clays, seawater Mg/Ca, and climate. Earth Planet. Sci. Lett. 416, 73–81. https://doi.org/10.1016/j.epsl.2015.01.003.

Hu, Z., Hu, W., Liu, C., Sun, F., Liu, Y., Li, W., 2019. Conservative behavior of Mg isotopes in massive dolostones: from diagenesis to hydrothermal reworking. Sediment. Geol. 381, 65–75. https://doi.org/10.1016/j.sedgeo.2018.12.007.

Huang, K.J., Shen, B., Lang, X.G., Tang, W.B., Peng, Y., Ke, S., Kaufman, A.J., Ma, H.R., Li, F.B., 2015. Magnesium isotopic compositions of the Mesoproterozoic dolostones: Implications for Mg isotopic systematics of marine carbonates. Geochim. Cosmochim. Acta 164, 333–351. https://doi.org/10.1016/j.gca.2015.05.002.

Illing, L.V., Wells, A.J., Taylor, J.C.M., 1965. Penecontemporary Dolomite in the Persian Gulf1. In: Pray, L.C., Murray, R.C. (Eds.), Dolomitization and Limestone Diagenesis. SEPM Society for Sedimentary Geology.

Jones, G.D., Rostron, B.J., 2000. Analysis of fluid flow constraints in regional-scale reflux dolomitization: constant versus variable-flux hydrogeological models. Bull. Can. Pet. Geol. 48, 230–245. https://doi.org/10.2113/48.3.230.

Kaczmarek, S.E., Gregg, J.M., Bish, D.L., Machel, H.G., Fouke, B.W., 2017. Dolomite, very high-magnesium calcite, and microbes—implications for the microbial model of dolomitization. In: Macneil, A.J., Lonnee, J., Wood, R. (Eds.), Characterization and Modeling of Carbonates–Mountjoy Symposium 1. SEPM (Society for Sedimentary Geology), pp. 7–20.

Kaczmarek, S.E., Sibley, D.F., 2011. On the evolution of dolomite stoichiometry and cation order during high-temperature synthesis experiments: an alternative model for the geochemical evolution of natural dolomites. Sediment. Geol. 240, 30–40. https://doi.org/10.1016/j.sedgeo.2011.07.003.

Kah, L.C., Grotzinger, J.P., James, N.P., 2000. Depositional $\delta^{18}O$ Signatures in Proterozoic Dolostones: Constraints on Seawater Chemistry and Early Diagenesis, Carbonate Sedimentation and Diagenesis in the Evolving Precambrian World. SEPM Society for Sedimentary Geology, pp. 345–360.

Ke, S., Teng, F.Z., Li, S.G., Gao, T., Liu, S.A., He, Y.S., Mo, X.X., 2016. Mg, Sr, and O isotope geochemistry of syenites from northwest Xinjiang, China: tracing carbonate recycling during Tethyan oceanic subduction. Chem. Geol. 437, 109–119. https://doi.org/10.1016/j.chemgeo.2016.05.002.

Land, L.S., 1985. The origin of massive dolomite. J. Geol. Educ. 33, 112–125.

Li, W.Q., Beard, B.L., Li, C.X., Xu, H.F., Johnson, C.M., 2015. Experimental calibration of Mg isotope fractionation between dolomite and aqueous solution and its geological implications. Geochim. Cosmochim. Acta 157, 164–181. https://doi.org/10.1016/j.gca.2015.02.024.

Li, W.Q., Bialik, O.M., Wang, X.M., Yang, T., Hu, Z.Y., Huang, Q.Y., Zhao, S.G., Waldmann, N.D., 2019. Effects of early diagenesis on Mg isotopes in dolomite: the roles of Mn(IV)-reduction and recrystallization. Geochim. Cosmochim. Acta 250, 1–17. https://doi.org/10.1016/j.gca.2019.01.029.

Lippmann, F., 1982. Stable and metastable solubility diagrams for the system $CaCO_3$–$MgCO_3$–H_2O at ordinary temperatures. Bull. Miner. 105, 273–279.

Lumsden, D.N., Caudle, G.C., 2001. Origin of massive dolostone: The Upper Knox model. J. Sediment. Res. 71, 400–409. https://doi.org/10.1306/2dc4094e-0e47-11d7-8643000102c1865d.

Machel, H.G., 2004. Concepts and models of dolomitization: a critical reappraisal. In: Braithwaite, C.J.R., Rizzl, G., Darke, G. (Eds.), The Geometryand Petrogenesisof Dolomite Hydrocarbon Reservoir. Geological Society, Special Publications, London, UK, pp. 7–63.

Mattes, B.W., Mountjoy, E.W., Zenger, D.H., Dunham, J.B., Ethington, R.L., 1980. Burial Dolomitization of the Upper Devonian Miette Buildup, Jasper National Park, Alberta 1. Concepts and Models of Dolomitization. SEPM Society for Sedimentary Geology.

Mavromatis, V., Meister, P., Oelkers, E.H., 2014. Using stable Mg isotopes to distinguish dolomite formation mechanisms: a case study from the Peru Margin. Chem. Geol. 385, 84–91. https://doi.org/10.1016/j.chemgeo.2014.07.019.

Mei, M.X., 2007. Sequence stratigraphic framework and its palaeogeographic setting for the Loushanguan Group dolostones of Cambrian in Upper Yangtze Region. J. Palaeogeogr. 9, 117–132.

Meister, P., Mckenzie, J.A., Bernasconi, S.M., Brack, P., 2013. Dolomite formation in the shallow seas of the Alpine Triassic. Sedimentology 60, 270–291. https://doi.org/10.1111/sed.12001.

Mresah, M.H., 1998. The massive dolomitization of platformal and basinal sequencesproposed models from the Paleocene, Northeast Sirte Basin, Libya. Sediment. Geol. 116, 199–226. https://doi.org/10.1016/S0037-0738(97)00107-3.

Ning, M., Huang, K., Lang, X., Ma, H., Yuan, H., Peng, Y., Shen, B., 2019. Can crystal morphology indicate different generations of dolomites? Evidence from magnesium isotopes. Chem. Geol. 516, 1–17. https://doi.org/10.1016/j.chemgeo.2019.04.007.

Peng, Y., Shen, B., Lang, X.G., Huang, K.J., Chen, J.T., Yan, Z., Tang, W.B., Ke, S., Ma, H.R., Li, F.B., 2016. Constraining dolomitization by Mg isotopes: a case study from partially dolomitized limestones of the middle Cambrian Xuzhuang Formation, North China. Geochem. Geophys. Geosyst. 17, 1109–1129. https://doi.org/10.1002/2015GC006057.

Petrash, D.A., Bialik, O.M., Bontognali, T.R.R., Vasconcelos, C., Roberts, J.A., Mckenzie, J.A., Konhauser, K.O., 2017. Microbially catalyzed dolomite formation: from near-surface to burial. Earth-Sci. Rev. 171, 558–582. https://doi.org/10.1016/j.earscirev.2017.06.015.

Purser, B., Tucker, M., Zenger, D., 1994. Problems, progress and future research concerning dolomites and dolomitization. In: Purser, B., Tucker, M., Zenger, D. (Eds.), Dolomites: A Volume in Honour of Dolomieu. Blackwell Scientific Publications, Cambridge, UK, pp. 1–20.

Roberts, J.A., Kenward, P.A., Fowle, D.A., Goldstein, R.H., González, L.A., Moore, D.S., 2013. Surface chemistry allows for abiotic precipitation of dolomite at low temperature. Proc. Natl. Acad. Sci. 110, 14540–14545. https://doi.org/10.1073/pnas.1305403110.

Shinn, E.A., Ginsburg, R.N., Lloyd, R.M., 1965. Recent supratidal Dolomite from Andros Island Bahamas. In: Pray, L.C., Murray, R.C. (Eds.), Special Publications of SEPM: Dolomitization and Limestone Diagenesis, pp. 112–123.

Teng, F.Z., 2017. Magnesium isotope geochemistry. Rev. Mineral. Geochem. 82, 219–287. https://doi.org/10.2138/rmg.2017.82.7.

Tipper, E., Galy, A., Gaillardet, J., Bickle, M., Elderfield, H., Carder, E., 2006. The magnesium isotope budget of the modern ocean: constraints from riverine magnesium isotope ratios. Earth Planet. Sci. Lett. 250, 241–253. https://doi.org/10.1016/j.epsl.2006.07.037.

Tipper, E.T., Gaillardet, J., Louvat, P., Capmas, F., White, A.F., 2010. Mg isotope constraints on soil pore-fluid chemistry: evidence from Santa Cruz, California. Geochim. Cosmochim. Acta 74, 3883–3896. https://doi.org/10.1016/j.gca.2010.04.021.

Vandeginste, V., Snell, O., Hall, M.R., Steer, E., Vandeginste, A., 2019. Acceleration of dolomitization by zinc in saline waters. Nat. Commun. 10, 1851. https://doi.org/10.1038/s41467-019-09870-y.

Vasconcelos, C., McKenzie, J.A., Bernasconi, S., Grujic, D., Tiens, A.J., 1995. Microbial mediation as a possible mechanism for natural dolomite formation at low temperatures. Nature 377, 220–222. https://doi.org/10.1038/377220a0.

Warren, J., 2000. Dolomite occurrence, evolution and economically important associations. Earth-Sci. Rev. 52, 1–81. https://doi.org/10.1016/S0012-8252(00)00022-2.

Wimpenny, J., Colla, C.A., Yin, Q.Z., Rustad, J.R., Casey, W.H., 2014. Investigating the behaviour of Mg isotopes during the formation of clay minerals. Geochim. Cosmochim. Acta 128, 178–194. https://doi.org/10.1016/j.gca.2013.12.012.

Yang, W., Kominz, M.A., 2003. Characteristics, stratigraphic architecture, and time framework of multi-order mixed siliciclastic and carbonate depositional sequences, outcropping Cisco Group (Late Pennsylvanian and Early Permian), Eastern Shelf, north-central Texas, USA. Sediment. Geol. 154, 53–87. https://doi.org/10.1016/S0037-0738(02)00100-8.